

# A new mouse model to explore the initiation, progression, and therapy of *BRAF*<sup>V600E</sup>-induced lung tumors

David Dankort,<sup>1</sup> Elena Filenova,<sup>1</sup> Manuel Collado,<sup>3</sup> Manuel Serrano,<sup>3</sup> Kirk Jones,<sup>2</sup> and Martin McMahon<sup>1,4</sup>

<sup>1</sup>Cancer Research Institute, Department of Cellular and Molecular Pharmacology, University of California, San Francisco Comprehensive Cancer Center, San Francisco, California 94143, USA; <sup>2</sup>Department of Pathology, University of California, San Francisco Comprehensive Cancer Center, San Francisco, California 94143, USA; <sup>3</sup>Spanish National Cancer Research Center (CNIO), Madrid 28029, Spain

**Mutationally activated *BRAF*<sup>V600E</sup> (*BRAF*<sup>VE</sup>) is detected in ~6% of human malignancies and promotes sustained MEK1/2–ERK1/2 pathway activation. We have designed *BRaf*<sup>CA</sup> mice to express normal *BRaf* prior to Cre-mediated recombination after which *BRaf*<sup>VE</sup> is expressed at physiological levels. *BRaf*<sup>CA</sup> mice infected with an Adenovirus expressing Cre recombinase developed benign lung tumors that only rarely progressed to adenocarcinoma. Moreover, *BRaf*<sup>VE</sup>-induced lung tumors were prevented by pharmacological inhibition of MEK1/2. *BRaf*<sup>VE</sup> expression initially induced proliferation that was followed by growth arrest bearing certain hallmarks of senescence. Consistent with *Ink4a/Arf* and *TP53* tumor suppressor function, *BRaf*<sup>VE</sup> expression combined with mutation of either locus led to cancer progression.**

Supplemental material is available at <http://www.genesdev.org>.

Received November 27, 2006; revised version accepted January 4, 2007.

The RAS-activated RAF–MEK–ERK mitogen-activated protein (MAP) kinase signaling pathway is directly implicated in the development of a wide variety of human malignancies. Although mutational activation of RAS in human cancer was first demonstrated in 1982, somatic activating mutations in *BRAF* were only detected in 2002 (Davies et al. 2002). Mutationally activated *BRAF* is detected in melanoma (70%), colorectal (15%), papillary thyroid (40%), ovarian (30%), and non-small-cell lung cancers (NSCLCs)(3%) (Davies et al. 2002; Zebisch and Troppmair 2006). Of the ~40 *BRAF* mutations identified to date, a T1799A transversion encoding constitutively active BRAF-V600E (*BRAF*<sup>VE</sup> hereafter) accounts for ~90% of all *BRAF* mutations (Wan et al. 2004). Mu-

tationally activated *BRAF*<sup>VE</sup> promotes the sustained activation of the ERK1/2 MAP kinases, pleiotropic regulators of the aberrant physiology of the cancer cell.

Lung cancer is the most prevalent cancer in the industrialized world and was responsible for ~165,000 deaths in the United States in 2005. Adenocarcinomas represent approximately one-half of all NSCLC subtypes. Despite its prevalence and characteristically high mortality rates, the cellular and genetic origins of the disease remain obscure. Mutational activation of *KRAS* or *BRAF* has been detected in ~25% of NSCLCs, and, while the majority of these harbor *KRAS* mutations, activating mutations in *BRAF* account for ~3% of all NSCLCs (Brose et al. 2002; Davies et al. 2002; Naoki et al. 2002). In addition, somatic mutations in the genes encoding the EGF receptor or *ERBB2*, both of which activate RAS signaling, are detected in ~13% of lung adenocarcinomas (Shigematsu and Gazdar 2006). Finally, ERK1/2 activation is associated with disease aggression, suggesting a more general role for this pathway in NSCLC pathogenesis (Vicent et al. 2004).

Here we describe mice carrying a genetically modified allele of *BRaf*, *BRaf*<sup>CA</sup>, which expresses normal *BRaf* prior to Cre-mediated recombination after which *BRaf*<sup>VE</sup> is expressed. *BRaf*<sup>VE</sup> expression in the lung elicited the growth of benign neoplastic adenomas, reminiscent of the effects of *KRAS*<sup>G12D</sup> expression (Jackson et al. 2001). Tumor formation was potently inhibited by pharmacological MEK1/2 inhibition. Evidence suggested that *BRaf*<sup>VE</sup>-induced lung tumors arose as a consequence of an initial burst of cell proliferation followed by an indolent phase, characterized by decreased proliferation accompanied by expression of senescence markers. Indeed, rarely did *BRaf*<sup>VE</sup>-induced adenomas display spontaneous progression to adenocarcinoma unless mice were deliberately engineered to lack the *TP53* or *Ink4a/Arf* tumor suppressor genes (TSGs).

## Results and Discussion

### Generation of *BRaf*<sup>CA</sup> mice by homologous recombination in embryonic stem (ES) cells

The development of new mouse models of human cancer places great emphasis on temporal and spatial control of oncogene expression, with particular attention paid to the levels of oncogene expression. This is especially important for *BRAF* since relatively small differences in RAF activity can promote quiescence, proliferation, or cell cycle arrest/senescence (Woods et al. 1997; Zhu et al. 1998). We sought to develop a mouse to accurately model the role of *BRaf*<sup>VE</sup> in cancer initiation, progression, and therapy with an emphasis on temporal and spatial control in tissues of interest. Using a suitably designed targeting vector (Fig. 1A), we used homologous recombination in ES cells to generate mice carrying a Cre-activated allele of *BRaf* (*BRaf*<sup>CA</sup>) (Fig. 1B). *BRaf*<sup>CA</sup> is designed to express normal *BRaf* prior to Cre-mediated recombination at which time *BRaf*<sup>VE</sup> expression is initiated at physiological expression levels and subject to normal patterns of alternate splicing and differential exon usage (Fig. 1C). By design, this model recapitulates the situation in human cells, where one copy of normal *BRAF* is converted by somatic mutation to *BRAF*<sup>VE</sup>. To discriminate the expression of the various *BRaf* mRNAs,

[Keywords: BRaf; mouse model; lung tumors; senescence]

<sup>4</sup>Corresponding author.

E-MAIL [mcmahon@cc.ucsf.edu](mailto:mcmahon@cc.ucsf.edu); FAX (415) 502-3179.

Article published online ahead of print. Article and publication date are online at <http://www.genesdev.org/cgi/doi/10.1101/gad.1516407>.

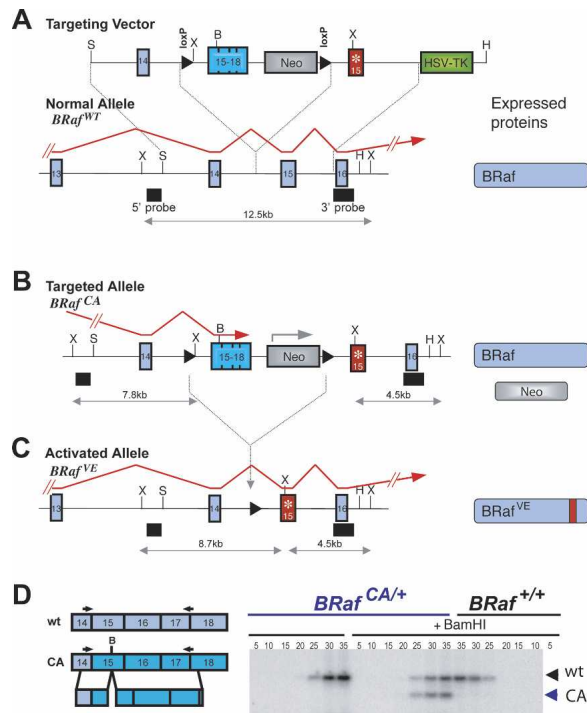


**Figure 1.** Schematic representation and generation of Cre-activated *BRaf* allele (*BRaf*<sup>CA</sup>). (A) The genomic *BRaf* locus (*BRaf*<sup>wt</sup>), the targeting vector used, and the proteins expressed from the locus are depicted. Red arrows depict fully processed *BRaf* mRNAs. External 5' and 3' probe locations and the size of XbaI restriction enzyme fragments are indicated. The modified exon 15 encoding V600E is indicated (\*). (B) The targeted *BRaf*<sup>CA</sup> allele and following Cre-mediated recombination, *BRaf*<sup>VE</sup> (C). (D) Semiquantitative RT-PCR analysis of targeted and wild-type ES cell-derived mRNAs using a radiolabeled reverse primer. PCR products amplified for the indicated numbers of cycles were treated with BamHI where indicated to distinguish *BRaf* transcripts. Expression of the *BRaf*<sup>CA</sup> allele was 98% that of endogenous *BRaf* mRNA.

silent restriction enzyme polymorphisms were incorporated into the exon 15 sequences of *BRaf*<sup>CA</sup> (BamHI, B) and *BRaf*<sup>VE</sup> (XbaI, X) (Fig. 1A–C).

Multiple correctly targeted ES cell clones were identified by Southern blotting (Supplemental Fig. 1A) and by RT-PCR analysis of *BRaf* and *BRaf*<sup>CA</sup> mRNA expression. The latter analysis confirmed that *BRaf* and *BRaf*<sup>CA</sup> mRNAs were expressed at the same level (Fig. 1D), whereas *BRaf*<sup>VE</sup> mRNA was not detected (data not shown). Two independent clones gave rise to chimeric mice that transmitted the *BRaf*<sup>CA</sup> allele through the germline. Breeding of *BRaf*<sup>CA/+</sup> mice to mice heterozygous for the CA allele, or a null allele, generated mice with all possible genotypes at normal Mendelian frequencies, demonstrating that the *BRaf*<sup>CA</sup> allele functions analogously to normal *BRaf* prior to Cre-mediated recombination (Supplemental Material).

#### *BRaf*<sup>VE</sup> expression in the lung elicits tumor formation

To test the utility of *BRaf*<sup>CA</sup> mice, we initiated expression of *BRaf*<sup>VE</sup> in the lungs by intranasal instillation of an adenovirus expressing Cre recombinase (Ad-Cre) (Fasbender et al. 1998). We chose this strategy for four reasons: (1) Mutationally activated *BRAF* has been described in human NSCLC (Zebisch and Troppmair 2006).

(2) The use of Ad-Cre provides temporal control over *BRaf*<sup>VE</sup> expression and therefore permits prospective evaluation of *BRaf*<sup>VE</sup> effects. (3) Ad-Cre titration allows control of the number of cells in which *BRaf*<sup>VE</sup> expression is initiated. (4) Others have previously described the effects of *Raf-1*- or Ad-Cre-induced *KRas*<sup>G12D</sup> expression in the lungs (Kerkhoff et al. 2000; Jackson et al. 2001; Tuveson et al. 2004).

Six- to eight-week-old wild-type or *BRaf*<sup>CA/+</sup> mice were administered with  $5 \times 10^7$  PFU (plaque-forming units) of either Ad-Cre or Ad- $\beta$ Gal. Mice were monitored for 7–8 wk, at which time all of the *BRaf*<sup>CA</sup> mice administered with Ad-Cre were euthanized due to evidence of labored breathing and general wasting. *BRaf*<sup>CA</sup> genomic rearrangement (Fig. 2A) and *BRaf*<sup>VE</sup> mRNA expression (Fig. 2B) were Cre-dependent and entirely restricted to the lung, as we detected no abnormalities or induction of *BRaf*<sup>CA</sup> somatic recombination in any other tissue analyzed. Lungs of *BRaf*<sup>VE</sup>-expressing mice displayed evidence of the formation of multiple lung tumors with an adenomatous morphology (Fig. 2C–H). Such lesions were not detected in *BRaf*<sup>CA</sup> mice even up to 6 mo after administration of a high dose of Ad- $\beta$ Gal or in wild-type mice infected with Ad-Cre. The effects of *BRaf*<sup>VE</sup> expression in the lung were highly penetrant in that all *BRaf*<sup>CA</sup> mice ( $n = 31$ ) treated with Ad-Cre ( $10^7$  PFU) developed lung tumors over the course of nine experiments. Moreover, induction of *BRaf*<sup>VE</sup> expression in the lung using a ubiquitously expressed, conditionally active CreER transgene (Guerra et al. 2003) elicited the formation of multiple lung tumors of the same type.

The cellular origins of human lung adenocarcinoma and adenomas are unclear. NSCLCs frequently express markers of Clara cells or alveolar type II pneumocytes (ATII). Indeed, it has been suggested that they arise from a common bronchio-alveolar stem cell (BASC) (Kim et al. 2005). To assess the properties of *BRaf*<sup>VE</sup>-induced tumors, immunohistochemical analyses to detect Clara Cell antigen (CCA/CC10) and Surfactant Protein-C (SP-C), a surface marker of ATII pneumocytes, were performed. Staining for CCA detected cells lining the bronchioles, but the *BRaf*<sup>VE</sup>-induced tumors were largely CCA negative (Fig. 2I,J). In contrast, the majority of cells within *BRaf*<sup>VE</sup>-induced tumors expressed SP-C, suggesting that they have properties of ATII pneumocytes (Fig. 2K,L). Furthermore, analysis of the earliest *BRaf*<sup>VE</sup>-induced lesions (2 wk after Ad-Cre) revealed them to express SP-C.

#### Requirement for *BRAF*<sup>VE</sup>-MEK-ERK activity for lung tumor formation

Clear genetic and biochemical evidence indicates that the MEK-ERK pathway plays an essential role in cancer cell proliferation, yet recent studies have suggested that alternate RAF-regulated pathways may exist (Chen et al. 2001). To address the effects of *BRaf*<sup>VE</sup> on canonical ERK signaling, we assessed phosphorylation of downstream effector proteins MEK1/2, ERK1/2, and the ERK-dependent phosphorylation of the Ets1/2 transcription factors. Indeed, using serial tissue sections, positive staining for all three of these surrogate markers of *BRaf*<sup>VE</sup> activity overlapped in all tested cases, demonstrating ERK MAP kinase activation (Fig. 3A,B; Supplementary Fig. 2A–C). It is reported that *KRas*<sup>G12D</sup>-induced lung tumors do not routinely display elevated pERK1/2 but display stress-

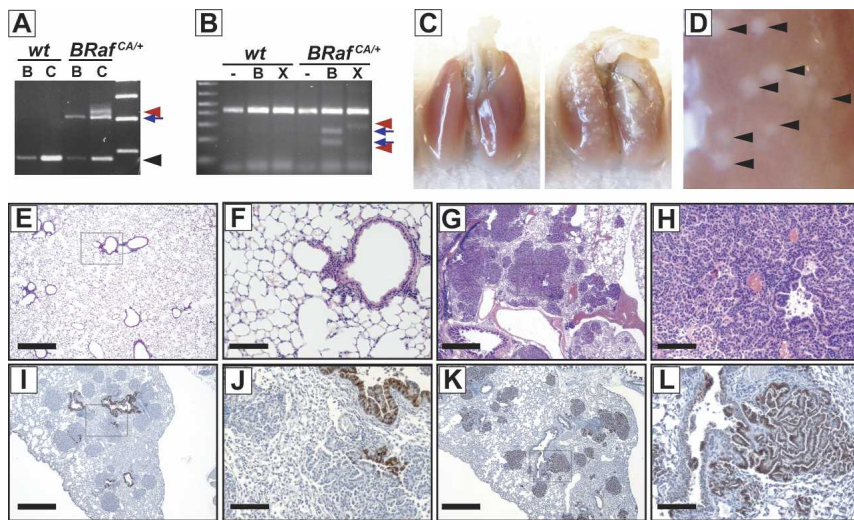


**Figure 2.** Expression of  $BRaf^{VE}$  in lung induces adenomas. (A) PCR detection of  $BRaf^{CA}$  rearrangement from lungs of  $BRaf^{+/+}$  (wt) or  $BRaf^{CA/+}$  mice infected with Ad- $\beta$ Gal (B) or Ad-Cre (C). The black arrowhead, blue arrow, and red arrowhead highlight the wild-type, the unrearranged  $BRaf^{CA}$ , and the  $BRaf^{VE}$  alleles, respectively. (B) Detection of  $BRaf^{VE}$  mRNA in  $BRaf^{CA/+}$  mice following Ad-Cre infection. Total lung RNA from  $BRaf^{+/+}$  (wt) or  $BRaf^{CA/+}$  mice isolated 8 wk after Ad-Cre infection ( $5 \times 10^7$  PFU) was subjected to RT-PCR analysis as in Figure 1D.  $BRaf^{CA}$  and  $BRaf^{VE}$  transcripts are distinguished through the use of restriction polymorphisms (BamHI, B; XbaI, X) with the diagnostic digestion products indicated by blue arrows and red arrowheads, respectively. (C–L)  $BRaf^{CA/+}$  mice were infected with  $5 \times 10^7$  PFU (C–H) or  $10^6$  PFU (I–L) of Ad-Cre intranasally and were analyzed 7 wk following infection. (C) Macroscopic lesions are present on the surface of  $BRaf^{CA/+}$  (right) and not wild-type (left) lungs. (E–H) Hematoxylin and eosin staining of histological sections of wild-type (E,F) or  $BRaf^{CA/+}$  (G,H). Note papillary adenomas in higher power magnification (H) and wide-scale involvement of lungs (G). (I,J) Adenomas stain negative for CCA (I,J) and positive for SP-C (K,L). Bars: F,H,I,L, 100  $\mu$ m; E,G,I,K, 500  $\mu$ m.

activated MAP kinase (SAPK/JNK) activation (Lee et al. 2002). Hence, to address the importance of MEK1/2 in  $BRaf^{VE}$ -induced tumor formation, we used PD0325901, a highly specific and selective MEK1/2 pharmacological inhibitor (a generous gift of Pfizer, Inc.). PD0325901 displays a nanomolar  $IC_{50}$  in cells and, unlike most protein kinase inhibitors, acts noncompetitively with its substrates (Sebolt-Leopold and Herrera 2004). Tumors were initiated in  $BRaf^{CA/+}$  mice by administration of  $5 \times 10^6$  PFU of Ad-Cre. Four weeks later, at a time when hyperplastic lung epithelium exists (Supplementary Fig. 2D), PD0325901, or the appropriate vehicle control, was administered daily by oral gavage for an additional 28 d (Fig. 3C). As expected, mice receiving the vehicle control displayed numerous lung tumors (Fig. 3D), whereas mice receiving PD0325901 were largely tumor free (Fig. 3E). These data indicate that the ability of  $BRaf^{VE}$  to elicit lung tumors is dependent on MEK1/2–ERK1/2 signaling. However, this does not eliminate the possibility that additional  $BRaf^{VE}$ -regulated pathways may contribute to tumor maintenance.

#### *BRaf<sup>VE</sup>-induced cell cycle arrest as a barrier to lung adenocarcinoma progression*

Induction of  $BRaf^{VE}$  expression by high dose Ad-Cre induced the formation of sufficiently large numbers of tumors that such mice rapidly succumbed to breathing difficulties and general wasting. In subsequent experiments, we used lower Ad-Cre doses to elicit smaller numbers of tumors to determine if such lesions would

display progression given sufficient time for additional events to occur. In addition, mice were euthanized at different times following Ad-Cre administration, and the histological appearance of the tumors was assessed. Lesions were characterized according to consensus criteria established by a panel of lung cancer biologists (Nikitin et al. 2004).

At early times after induced  $BRaf^{VE}$  expression, we detected evidence of epithelial hyperplasia (classified as 1.1.1.1) arising within the terminal bronchioles and within the central lung parenchyma. This hyperplastic epithelium displayed papillary excrescences; however, at early time points (2–4 wk), there was no nodule formation (Fig. 4A). Papillary adenomas (1.2.1.2.2) were detected 6–8 wk after  $BRaf^{VE}$  expression and appeared to increase in number and size. These lesions were bronchiolocentric, but did not appear to involve the terminal bronchioles. Rather, the lesions appeared to arise in alveolar ducts and expand outward and around bronchioles (Fig. 4B). At later times (~14 wk) after  $BRaf^{VE}$  induction, we detected changes in the papillary adenomas such that they appeared to undergo alterations at their periphery, changing to a more solid architectural appearance (Fig. 4C). The cells also displayed additional morphologic alterations where the cytoplasm became more abundant and eosinophilic. This is consistent with the appearance of mixed papillary and solid adenomas (1.2.1.2.3). It is striking that the  $BRaf^{VE}$ -induced lung adenomas formed rapidly (6–8 wk), but did not appear to grow beyond ~900  $\mu$ m in diameter. Moreover, we rarely detected spontaneous progression to adenocarcinoma in these mice. To date, only two out of 57  $BRaf^{CA}$  mice possessing adenomas displayed focal adenocarcinomas at the time of necropsy (Fig. 4D). The adenocarcinoma cells in these two mice displayed nuclear enlargement, hyperchromasia, and contour irregularities. The cells were arranged in solid sheets, histologically consistent with adenocarcinoma (1.2.3.2). Thus, expression of  $BRaf^{VE}$  appears sufficient to rapidly induce benign lung tumors that only rarely progress to adenocarcinoma, suggesting that additional events are required for cancer progression.

By a similar strategy, others assessed the effects of  $BRaf^{VE}$  expression in the hematopoietic system. In this case,  $BRaf^{VE}$  elicits hematopoietic dysplasia with characteristics of histiocytic sarcoma (Mercer et al. 2005). In this model,  $BRaf^{VE}$  expression is uniformly lethal due to bone marrow failure, but mice do not die due to acute myeloid leukemia, suggesting that  $BRaf^{VE}$  induces a pre-malignant myelodysplastic state. It is interesting to note that the consequences of induced  $BRaf^{VE}$  lung expression bear both interesting similarities and differences in comparison to those reported for  $KRas^{G12D}$  (Jackson et al. 2001). Ad-Cre-induced expression of  $KRas^{G12D}$  in the lungs of  $KRas^{LSL}$  mice leads initially to development of

display progression given sufficient time for additional events to occur. In addition, mice were euthanized at different times following Ad-Cre administration, and the histological appearance of the tumors was assessed. Lesions were characterized according to consensus criteria established by a panel of lung cancer biologists (Nikitin et al. 2004).

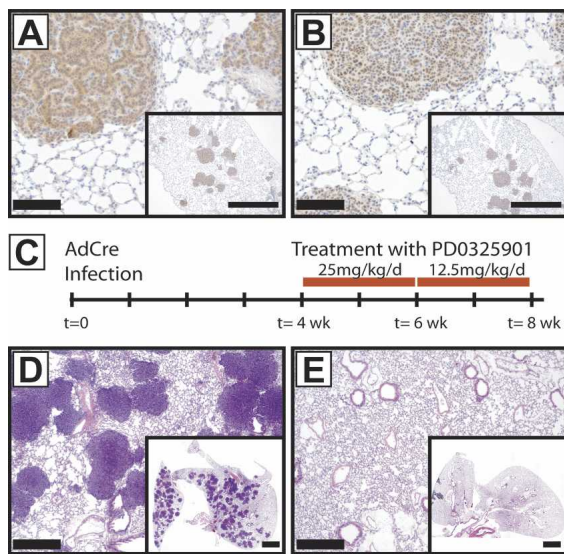


**Figure 3.** MEK1/2 dependency of  $BRAF^{VE}$ -induced adenoma formation. (A,B) Adenomas stain positive for active MEK (A) and active ERK (B). (C) Time line of PD0325901 treatment.  $BRAF^{CA}$  mice infected with Ad-Cre ( $5 \times 10^6$  PFU) were grouped randomly into one of two arms: One arm received PD0325901, and the other received vehicle control. Drug treatment was initiated 4 wk after initial infection of mice and was sustained at the indicated concentrations for 28 d. Eight weeks post-infection, all mice receiving vehicle develop multiple adenomas (D), whereas no mouse treated with PD0325901 developed adenomas (E). (Insets) Lower magnification. Bars: A,B,D,E, 100  $\mu$ m; A,B, insets, 1 mm; E,F, insets, 2 mm.

atypical adenomatous hyperplasia (AAH,  $\sim 2$  wk) that progresses to adenoma ( $\sim 6$  wk). Interestingly, the major difference appears to be that expression of  $KRAS^{G12D}$  in the lung leads to more rapid and consistent progression to adenocarcinoma than that elicited by  $BRAF^{VE}$ . These data suggest that either additional KRas effector pathways are required for cancer progression or that  $BRAF^{VE}$ -induced adenomas are more highly constrained from progression.

Oncogene-induced cell cycle arrest with features of senescence (OIS) is reported to be a cellular defense mechanism restraining the proliferation of normal cells in response to inappropriate activation of RAS or its signaling effectors (Collado et al. 2005; Michaloglou et al. 2005). Recently, it was reported that  $KRAS^{G12D}$ -induced lung tumors are arrested in the cell cycle and express OIS markers (Collado et al. 2005). To determine if  $BRAF^{VE}$ -induced lung tumors display evidence of OIS, tissue sections from lungs harvested at different times after  $BRAF^{VE}$  expression were stained for markers of cell proliferation (phospho-histone H3, Ki67, or BrdU incorporation) and for OIS markers (SA- $\beta$ Gal, p19<sup>ARF</sup>, Dec1). In hyperplastic lung tissues and in tumors induced at early times after  $BRAF^{VE}$  expression, a high percentage of cells stain positive for Ki67 (Fig. 4E,F), phospho-histone H3, and BrdU incorporation. However, in tumors observed at later times, the percentage of Ki67-positive cells is dramatically decreased even though the  $BRAF^{VE}$ -MEK-ERK signaling pathway remains active in these cells (Figs. 3A,B, 4G). Further analysis of adenomatous lesions revealed that they were positive for expression of p19<sup>ARF</sup> and Dec1 (Fig. 4I,J). p19<sup>ARF</sup> expression was detected in  $\sim 15\%$  of tumor cells with staining localized to nucleoli, a pattern consistent with previous data (Weber et al.

1999). While these markers of OIS were readily detected, these adenomas were largely negative for SA- $\beta$ Gal activity (Fig. 4K). In the  $BRAF^{VE}$ -induced adenocarcinomas found in the two mice displaying tumor progression, however, a very high rate of Ki67 staining was observed (Fig. 4H). These data are consistent with the hypothesis that sustained activation of  $BRAF^{VE}$  promotes an initial period of cell proliferation followed by cell cycle arrest constraining further tumor progression.

#### *BRAF<sup>VE</sup> cooperates with TSG loss to promote adenocarcinoma formation*

If  $BRAF^{VE}$ -induced senescence is a barrier to lung carcinogenesis, then  $BRAF^{VE}$  expression combined with loss of TSG expression should lead to cancer progression. To this end, we crossed  $BRAF^{CA}$  mice to obtain mice homozygous for floxed alleles of either  $TP53$  or  $Ink4a/Arf$ . These mice express normal levels of the various TSGs until the modified alleles undergo Cre-mediated deletion of critical exons. Concomitant loss of  $TP53$  led to increased proliferation at  $\sim 8$  wk post-infection with Ad-Cre when compared with  $BRAF^{CA/+}$ ;  $TP53^{+/+}$  mice (Fig. 4L,M,O,P). Histological analyses of lungs from  $BRAF^{CA/+}$ ;  $TP53^{lox/lox}$  mice revealed rapid cancer progression (Fig. 4L,M,R) and showed nodules composed of central papillary structures with solid peripheral areas (similar to older  $BRAF^{CA/+}$  mice) consistent with formation of mixed adenomas (1.2.1.2.3). Several small airways also displayed papillary hyperplasia, which was never observed in  $BRAF^{CA/+}$  mice. In each case analyzed ( $n = 5$ ), mice lacking  $TP53$  function displayed an increased proliferative index (Fig. 4P; Supplementary Fig. 3), and cells displayed altered nuclear morphology (Fig. 4S). Collections of cells with enlarged nuclei stained positive for Ki67, indicating ongoing proliferation (Supplementary Fig. 3A–D). Significantly, at  $\sim 8$  wk post-infection, all  $BRAF^{+/+}$  mice homozygous for the  $TP53^{lox}$  allele had a normal lung phenotype (data not shown). Upon euthanasia, 2/5  $BRAF^{CA/+}$ ;  $TP53^{lox/lox}$  mice displayed prominent adenocarcinomas (Fig. 4R) composed of glandular structures lined by highly atypical cells with nuclear enlargement, hyperchromasia, and contour irregularities and displayed prominent nucleoli (Fig. 4S). The adenocarcinomas possessed large areas of necrosis and showed evidence of vascular and lymphatic invasion. This is significant, as we have not detected adenocarcinoma in any  $BRAF^{CA}$  mice prior to 40 wk of age ( $n = 55$ ).

Similarly,  $BRAF^{VE}$  expression in an  $Ink4a/Arf^{lox/lox}$  background led to scattered papillary adenomas with evidence of subpleural nodules harboring cords of atypical cells trapped within regions of mesenchymal proliferation. 2/4  $BRAF^{CA/+}$ ;  $Ink4a/Arf^{lox/lox}$  mice contained multiple lung tumors with a classical bronchioloalveolar component and, when tumor cells were present, growing along alveolar septa without architectural destruction. This pattern is peculiar and is not categorized in the recent classification scheme but displays phenotypic similarities to human bronchioloalveolar carcinoma. Ki67 staining demonstrates that these lesions display increased proliferation relative to  $BRAF^{VE}$ -induced adenomas (Fig. 4Q).

The data presented here provide support for the hypothesis that oncogenic  $BRAF$  can provoke cell cycle arrest accompanied by induction of some, but not all, markers of OIS (Zhu et al. 1998; Collado et al. 2005).

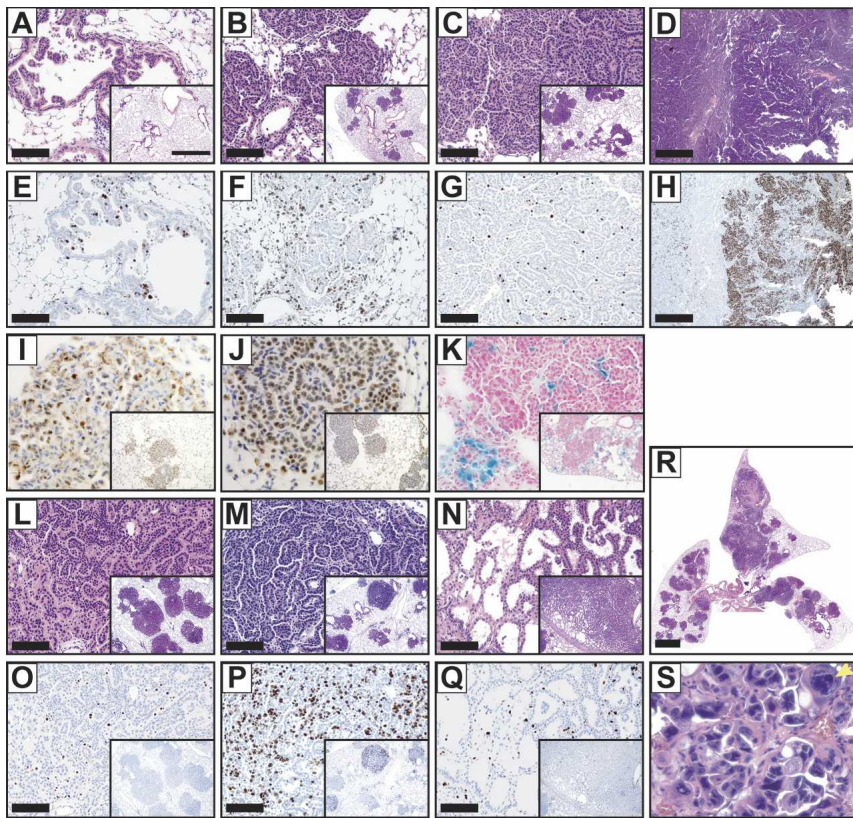


**Figure 4.** Sustained *BRAF*<sup>VE</sup> expression induces a proliferative arrest with hallmarks of oncogene-induced senescence. (A–D) Lung histology was analyzed from *BRAF*<sup>CA</sup> mice at 4 wk (A), 6 wk (B), 14 wk (C), and 41 wk (D) post-infection with 10<sup>7</sup> PFU (A–C) or 10<sup>5</sup> PFU (D) of Ad-Cre. Note that the hyperplastic tissue in A was observed as early as 14 d post-infection with high doses of Ad-Cre. (E–H) Ki67 immunochemical staining of lung sections at 4 wk (E), 6 wk (F), 8 wk (G), and 41 wk (H) post-infection using serial section of those depicted in A–D. (I–K) *BRAF*<sup>VE</sup>-induced adenomas express p19<sup>ARF</sup> (I) and Dec1 (J) and are negative for SA-βGal (K). (L–S) *BRAF*<sup>CA</sup> mice (L,O) and those homozygous for conditional alleles of *TP53* (M,P,R,S) or *Ink4a/Arf* (N,Q) were analyzed at 7 wk (R,S), 9 wk (L,M,O,P) or 14 wk (N,Q) post-infection with Ad-Cre. (O–Q) Ki67 immunochemical staining of serial lung sections from L–N. (R,S) Low-powered (R) and high-powered (S) views of *BRAF*<sup>CA</sup>; *TP53*<sup>lox/lox</sup> lungs demonstrate the extent of lesions and disordered morphology, enlarged size (yellow arrow), and heterochromatic staining of nuclei. Bars, A–C, E–G, L–Q, 100 μm; D, H, 500 μm; insets, 1 mm; R, 2 mm.

That *KRAS*<sup>G12D</sup> (Jackson et al. 2005) or *BRAF*<sup>VE</sup> can cooperate with loss of TSGs believed to mediate OIS is further, albeit circumstantial, evidence that OIS may serve as a bona fide tumor-suppressive mechanism in vivo. However, there remains at least one conundrum in this hypothesis. Adenomas that arise from expression of *KRAS*<sup>G12D</sup> or *BRAF*<sup>VE</sup> were initiated by oncogene activation in a single cell that subsequently underwent ~15–20 population doublings to give rise to an adenoma. Clearly then, the initial response to *KRAS*<sup>G12D</sup> or *BRAF*<sup>VE</sup> expression is not cell cycle arrest but a dramatic induction of cell proliferation. However, at some time temporally distinct from oncogene activation, mechanisms that promote cell cycle arrest/senescence are engaged. This interpretation is consistent with the observation that *BRAF*<sup>VE</sup>-induced melanocytic nevi are clonal, having undergone multiple rounds of proliferation (Pollock et al. 2003), but eventually undergo senescence (Michaloglou et al. 2005). One possibility is that these biologically distinct outcomes reflect differences in the level of oncogene expression/activation at different stages of tumor progression. Alternatively, secondary signals may coop-

erate with *KRAS*<sup>G12D</sup> or *BRAF*<sup>VE</sup> to initiate and/or maintain the OIS program. These observations contrast with those in cultured cells, where activation of RAF robustly induces p16<sup>INK4A</sup> and irreversible cell cycle arrest/senescence within 12–24 h and in the absence of any initial cell proliferation (Zhu et al. 1998). While in vitro culture conditions may cooperate with RAF in the induction of senescence, the nature of the secondary trigger for OIS in vivo remains a key unanswered question.

## Materials and methods

### Generation of a conditionally active *BRAF* allele

DNA encompassing mouse *BRAF* exons 14–16 was modified such that exon 16 was replaced with a HSV-thymidine kinase cassette. A LoxP-flanked cassette containing the 3' 382 base pairs (bp) of intron 14, the human *BRAF* cDNA containing exons 15–18, the mouse *BRAF* polyadenylation sequences, and a PGK-neo cassette was inserted into intron 14 upstream of a modified exon 15 that encodes BRAF<sup>V600E</sup> and a silent XbaI restriction site polymorphism. The details of construction, Southern blotting, and RNA analysis are available as Supplemental Material.

### Mice used in this study

Mice carrying conditional alleles of *TP53* or *Ink4a/Arf* were genotyped as described in the Supplemental Material. *BRAF*<sup>CA</sup> mouse genotypes were determined by standard PCR of tail DNA with primer pair AD (AD FwdA1, 5'-TGAGTATTTTGTGGCAACTGC-3'; and AD RevB1, 5'-CTCTGCTGGGAAAGCGGC-3') to produce diagnostic PCR products of 185 bp, 308 bp, and 335 bp for *BRAF*, *BRAF*<sup>CA</sup>, and the *BRAF*<sup>VE</sup> alleles, respectively.

### Adenoviral Cre delivery

Ad-Cre and Ad-βGal were purified and titered by standard means (Viraquest), and 10<sup>5</sup> to 5 × 10<sup>7</sup>

PFU were administered to the nasal septum of 6- to 8-wk-old mice by intranasal instillation as a calcium phosphate precipitate (Fasbender et al. 1998).

### Immunohistochemistry

Animals were euthanized at the specified times or upon display of visible signs of disease. Lung tissues were prepared through standard techniques. Immunostaining was performed as described in the Supplemental Material using antibodies to CC10 (1:800); SP-C (Santa Cruz Biochemicals; 1:200); pMEK (Cell Signaling; 1:50); pERK (Cell Signaling; 1:100); and Ki67 (NeoMarkers; 1:200) with secondary antibodies and detection kits from DakoCytomation.

## Acknowledgments

We thank Allan Balmain, Anton Berns, David Carretto, Ron DePinho, Byron Hann, Takashi Hirano, Nigel Killeen, Akiko Kobiyashi, Tyler Jacks, Leisa Johnson, Jennifer LeCouter, Anil Mukherjee, Daniel Murphy, Judith Sebolt-Leopold, and the UCSF transgenic, preclinical therapeutics, and mouse pathology core facilities for mice, materials, reagents, technical assistance, and advice. We thank Mike Fried and members of the Stokoe, Balmain, and McMahon laboratories for discussion. We acknowledge financial support from the General Motors Cancer Research Scholars Program (D.D.), Mouse Models of Human Cancer Consortium CA084244, and U.C. Discovery Grant (M.M.).

## References

- Brose, M.S., Volpe, P., Feldman, M., Kumar, M., Rishi, I., Gerrero, R., Einhorn, E., Herlyn, M., Minna, J., Nicholson, A., et al. 2002. BRAF and RAS mutations in human lung cancer and melanoma. *Cancer Res.* **62**: 6997–7000.
- Chen, J., Fujii, K., Zhang, L., Roberts, T., and Fu, H. 2001. Raf-1 promotes cell survival by antagonizing apoptosis signal-regulating kinase 1 through a MEK–ERK independent mechanism. *Proc. Natl. Acad. Sci.* **98**: 7783–7788.
- Collado, M., Gil, J., Efeyan, A., Guerra, C., Schuhmacher, A.J., Barradas, M., Benguria, A., Zaballos, A., Flores, J.M., Barbacid, M., et al. 2005. Tumour biology: Senescence in premalignant tumours. *Nature* **436**: 642.
- Davies, H., Bignell, G.R., Cox, C., Stephens, P., Edkins, S., Clegg, S., Teague, J., Woffendin, H., Garnett, M.J., Bottomley, W., et al. 2002. Mutations of the BRAF gene in human cancer. *Nature* **417**: 949–954.
- Fasbender, A., Lee, J.H., Walters, R.W., Moninger, T.O., Zabner, J., and Welsh, M.J. 1998. Incorporation of adenovirus in calcium phosphate precipitates enhances gene transfer to airway epithelia in vitro and in vivo. *J. Clin. Invest.* **102**: 184–193.
- Guerra, C., Mijimolle, N., Dhawahir, A., Dubus, P., Barradas, M., Serrano, M., Campuzano, V., and Barbacid, M. 2003. Tumor induction by an endogenous K-ras oncogene is highly dependent on cellular context. *Cancer Cell* **4**: 111–120.
- Jackson, E.L., Willis, N., Mercer, K., Bronson, R.T., Crowley, D., Montoya, R., Jacks, T., and Tuveson, D.A. 2001. Analysis of lung tumor initiation and progression using conditional expression of oncogenic K-ras. *Genes & Dev.* **15**: 3243–3248.
- Jackson, E.L., Olive, K.P., Tuveson, D.A., Bronson, R., Crowley, D., Brown, M., and Jacks, T. 2005. The differential effects of mutant p53 alleles on advanced murine lung cancer. *Cancer Res.* **65**: 10280–10288.
- Kerckhoff, E., Fedorov, L.M., Siefken, R., Walter, A.O., Papadopoulos, T., and Rapp, U.R. 2000. Lung-targeted expression of the c-Raf-1 kinase in transgenic mice exposes a novel oncogenic character of the wild-type protein. *Cell Growth Differ.* **11**: 185–190.
- Kim, C.F., Jackson, E.L., Woolfenden, A.E., Lawrence, S., Babar, I., Vogel, S., Crowley, D., Bronson, R.T., and Jacks, T. 2005. Identification of bronchioalveolar stem cells in normal lung and lung cancer. *Cell* **121**: 823–835.
- Lee, H.Y., Suh, Y.A., Lee, J.I., Hassan, K.A., Mao, L., Force, T., Gilbert, B.E., Jacks, T., and Kurie, J.M. 2002. Inhibition of oncogenic K-ras signaling by aerosolized gene delivery in a mouse model of human lung cancer. *Clin. Cancer Res.* **8**: 2970–2975.
- Mercer, K., Giblett, S., Green, S., Lloyd, D., DaRocha Dias, S., Plumb, M., Marais, R., and Pritchard, C. 2005. Expression of endogenous oncogenic <sup>V600E</sup>B-raf induces proliferation and developmental defects in mice and transformation of primary fibroblasts. *Cancer Res.* **65**: 11493–11500.
- Michaloglou, C., Vredeveld, L.C., Soengas, M.S., Denoyelle, C., Kuilman, T., van der Horst, C.M., Majoor, D.M., Shay, J.W., Mooi, W.J., and Peepers, D.S. 2005. BRAF<sup>E600</sup>-associated senescence-like cell cycle arrest of human naevi. *Nature* **436**: 720–724.
- Naoki, K., Chen, T.H., Richards, W.G., Sugarbaker, D.J., and Meyerson, M. 2002. Missense mutations of the BRAF gene in human lung adenocarcinoma. *Cancer Res.* **62**: 7001–7003.
- Nikitin, A.Y., Alcaraz, A., Anver, M.R., Bronson, R.T., Cardiff, R.D., Dixon, D., Fraire, A.E., Gabrielson, E.W., Gunning, W.T., Haines, D.C., et al. 2004. Classification of proliferative pulmonary lesions of the mouse: Recommendations of the Mouse Models of Human Cancers Consortium. *Cancer Res.* **64**: 2307–2316.
- Pollock, P.M., Harper, U.L., Hansen, K.S., Yudt, L.M., Stark, M., Robbins, C.M., Moses, T.Y., Hostetter, G., Wagner, U., Kakareka, J., et al. 2003. High frequency of BRAF mutations in nevi. *Nat. Genet.* **33**: 19–20.
- Sebolt-Leopold, J.S. and Herrera, R. 2004. Targeting the mitogen-activated protein kinase cascade to treat cancer. *Nat. Rev. Cancer* **4**: 937–947.
- Shigematsu, H. and Gazdar, A.F. 2006. Somatic mutations of epidermal growth factor receptor signaling pathway in lung cancers. *Int. J. Cancer* **118**: 257–262.
- Tuveson, D.A., Shaw, A.T., Willis, N.A., Silver, D.P., Jackson, E.L., Chang, S., Mercer, K.L., Grochow, R., Hock, H., Crowley, D., et al. 2004. Endogenous oncogenic K-ras(G12D) stimulates proliferation and widespread neoplastic and developmental defects. *Cancer Cell* **5**: 375–387.
- Vicent, S., Lopez-Picazo, J.M., Toledo, G., Lozano, M.D., Torre, W., Garcia-Corchon, C., Quero, C., Soria, J.C., Martin-Algarra, S., Manzano, R.G., et al. 2004. ERK1/2 is activated in non-small-cell lung cancer and associated with advanced tumours. *Br. J. Cancer* **90**: 1047–1052.
- Wan, P.T., Garnett, M.J., Roe, S.M., Lee, S., Niculescu-Duvaz, D., Good, V.M., Jones, C.M., Marshall, C.J., Springer, C.J., Barford, D., et al. 2004. Mechanism of activation of the RAF–ERK signaling pathway by oncogenic mutations of B-RAF. *Cell* **116**: 855–867.
- Weber, J.D., Taylor, L.J., Rousset, M.F., Sherr, C.J., and Bar-Sagi, D. 1999. Nucleolar Arf sequesters Mdm2 and activates p53. *Nat. Cell Biol.* **1**: 20–26.
- Woods, D., Parry, D., Cherwinski, H., Bosch, E., Lees, E., and McMahon, M. 1997. Raf-induced proliferation or cell cycle arrest is determined by the level of Raf activity with arrest mediated by p21Cip1. *Mol. Cell Biol.* **17**: 5598–5611.
- Zebisch, A. and Troppmair, J. 2006. Back to the roots: The remarkable RAF oncogene story. *Cell. Mol. Life Sci.* **63**: 1314–1330.
- Zhu, J., Woods, D., McMahon, M., and Bishop, J.M. 1998. Senescence of human fibroblasts induced by oncogenic Raf. *Genes & Dev.* **12**: 2997–3007.